Soft-Core Attractive Model Fluid: Structure, Thermodynamics and Inter-colloidal Solvation Force[†]

Andrej Lajovic and Andrej Jamnik*

*University of Ljubljana, Faculty of Chemistry and Chemical Technology, Aškerčeva 5,
SI-1001 Ljubljana, Slovenia*

* Corresponding author: E-mail: andrej.jamnik @fkkt.uni-lj.si

Received: 25-05-2007

[†]Dedicated to Prof. Dr. Jože Škerjanc on the occasion of his 70th birthday

Abstract

Canonical and grand canonical Monte Carlo simulations are used to study a system of spherical particles interacting via a discontinuous potential combining a repulsive square soft core and an attractive square well. This, so-called core-softened (CS) potential fluid is known to have both a gas-liquid critical point and a liquid-liquid critical point separating high density liquid (HDL) and low density liquid (LDL) phases. First, the spatial correlations and thermodynamic properties of homogeneous and inhomogeneous CS fluid are investigated. Using open ensemble simulation we study an equilibrium distribution of the CS fluid between the homogeneous phase and the planar pores mimicking the real porous material. The bulk radial distribution function displays discontinuities at the distances coinciding with the ranges of the successive repulsive and attractive parts in the CS potential function. The density profiles of confined CS fluid show the shapes arising from the interplay among the steric effects and the competition between the repulsive and attractive parts of the CS potential. Then, the effective force between a pair of big colloidal spheres immersed in a sea of small spheres interacting via CS potential is explored. The big-small interactions are modeled as hard core pair potentials with attractive or repulsive Yukawa tail leading to the accumulation repulsion and depletion attraction between the two colloids, respectively. For this purpose we apply a special simulation technique based on a separate sampling of the contributions arising from the Yukawa tail and hard-core (collision) parts of the big-small interaction potential to the total force between the colloidal particles.

Keywords: Monte Carlo simulation, soft-core potential, Yukawa potential, potential of mean force, solvation interaction

1. Introduction

More than three decades ago, Stell and Hemmer proposed the possibility of a second critical point in addition to the normal liquid-gas critical point for one-dimensional systems whose pairwise potentials possess a region of negative curvature in their repulsive core.[1,2] These so-called core-softened (CS) potentials exhibit a repulsive hard core plus a softening region, which can be a linear or non-linear repulsive ramp, a shoulder, a double (or multiple) attractive well, or a combination of all these features.[1,3–11] These models were created with the purpose of constructing simple two-body isotropic potential capable of describing some aspects of anomalous behavior of water and some other fluids,[12–14] like the maximum in density as a function of temperature and the increase of the isothermal compressibility upon cooling. It has been proposed some time ago that these anomalies might be associated with a critical point at the terminus of a liquid-liquid line in the unstable supercooled liquid region.[15–17] Soft-core model potentials may therefore reproduce the density anomaly of water. Namely, at lower pressures and temperatures, the neighboring molecules are separated by the distances coinciding with the range of attractive potential well to minimize the energy. At higher temperatures, the particles penetrate into the energetically less favorable softened core to gain more entropy thus giving rise to an anomalous contraction upon heating. As predicted by hypernetted chain integral equation and computer simulations[18,19,11] these potentials possess a second critical point also in three dimensions for a narrow range of potential parameters and on condition that the height of repulsive shoulder is larger than the depth of the attractive potential well.

In our previous paper,[20] we investigated a three-dimensional potential, which besides the hard-core repulsion incorporated a double square-well attractive interaction. On the contrary to the CS potentials exhibiting repulsive ramp or shoulder in a softening region, which gives rise to a second liquid-liquid critical point, the model system comprising a fully attractive softening region of the potential function has only the gas-liquid critical point. We have determined the gas-liquid phase diagrams for various ranges of the individual square wells of the potential utilizing discrete molecular dynamics (DMD) simulation, which enables a treatment of the discontinuous stepwise potentials. These diagrams served as a basis for the appropriate choice of bulk density and potential parameters, at which we studied the thermodynamic properties and structural features of this model fluid in homogeneous phase and the inhomogeneous structure of the same fluid subjected to various external fields originating from the presence of various spatial constrains. For the latter, we have chosen a hard flat interface and a closed spherical surface mimicking a spherical cavity. In the present work we extend this previous investigation to a CS model system incorporating soft-core repulsive interactions in the potential function. Recently, Skibinsky et al[21] reported extensive systematic DMD studies of the phase diagrams for CS fluid. In the work of Ref. 21 the authors found that this potential has a phase diagram with a liquid-liquid critical point for a wide range of parameters. In this present study we therefore use these diagrams to read the range of parameters where the bulk CS fluid represents the one-phase system. The thermodynamic properties and homogeneous and inhomogeneous structures of the CS fluid at one set of potential parameters and various densities corresponding to state points located in a 'safe' one-phase region of the phase diagram are then determined by a grand canonical ensemble Monte Carlo (GCEMC) simulation.

The structure of the molecular solvent in the interface among large (macro)particles mimicking colloidal solute is responsible for the inter-colloidal solvation force, often called also as solvent mediated or structural force. As colloidal particles take part in various chemical and biological reactions, knowledge of the solvation force is also of great practical importance. The solvent mediated forces between the colloidal macro-particles in suspensions, stemming from the depletion and accumulation effects, are therefore of longstanding and continuing interest as they play an important role in many industrial and biological applications. For example, the depletion effect may lead to phase separation of colloidal dispersions and protein crystallization.[22–24] For this reason, in addition to the structural study of the pure CS fluid, we perform also extensive canonical Monte Carlo (MC) simulations of a binary mixture comprising of two macrospheres (solute) and a microsphere background fluid (solvent) interacting via CS potential, to determine the effective force between a pair of colloidal particles. In the present work, the big-small interactions are modeled as

hard core pair potentials with attractive or repulsive Yukawa tail mimicking lyophilic and lyophobic colloids, respectively, and leading to the repulsive and attractive (entropic) forces between the colloidal particles. For this purpose we apply a simulation technique developed by Wu et al[25,26] for MC sampling of the hard-sphere collision force, which arises from the collisions of colloidal particles with the adjacent molecules of the solvent.

2. Models and Monte Carlo Simulations

2. 1. Models

First, we study the thermodynamic and structural properties of homogeneous one-component system of particles interacting via a core-softened (CS) pair potential

$$
\phi(r) = \infty, \qquad r < \sigma
$$
$$
= \lambda\varepsilon, \qquad \sigma < r < b
$$
$$
= -\varepsilon, \qquad b < r < c \qquad (1)
$$
$$
= 0, \qquad r > c
$$

This 3D isotropic potential has a hard core (infinite repulsion) at distance σ, a repulsive soft core of width $b - \sigma$ and energy $\lambda\varepsilon > 0$, and an attractive square well of width $c - b$ and energy $-\varepsilon < 0$.[9,18] Though this potential is discontinuous, it resembles the model potentials for complex fluids including colloids, protein solutions, star polymers,[27–33] and, as mentioned in the Introduction, is similar to pair potentials proposed for water.[29]

Further, we investigate the structure of the CS fluid near a planar interface and confined in planar pore. The external potentials ϕ_{ext} due to the presence of these spatial constrains read:

$$
\phi_{ext}(x) = \begin{cases} 0 & x > \frac{1}{2}\sigma \\ \infty & \text{otherwise} \end{cases} \qquad (2)
$$

for a single hard wall, and

$$
\phi_{ext}(x) = \begin{cases} 0 & \frac{1}{2}\sigma < x < H - \frac{1}{2}\sigma \\ \infty & \text{otherwise} \end{cases} \qquad (3)
$$

for a planar slit with two plane hard walls situated at $x = 0$ and $x = H$, respectively, where x is the coordinate perpendicular to the wall(s).

The effective force between colloidal particles is calculated using a simple model, which comprises a pair of big spheres (solute) of the diameter σ_b immersed in a sea of smaller spheres (solvent) with the diameter $\sigma_s = \sigma$ and interacting among themselves through the CS potential given by the Eq. 1. As the macrosphere component is treated at effectively infinite dilution the solvent contribu-

tion to the total inter-colloidal force is extracted. Throughout, the big-big interaction potential ϕ_{bb} (r) is set to zero. The big-small interactions are modeled as hard-core Yukawa pair potential

$$\phi_{bs}(r) = \begin{cases} \varepsilon_{bs}\sigma_{bs}\exp\left[-\kappa_{bs}\left(r-\sigma_{bs}\right)/\sigma_{bs}\right]/r \\ \infty \qquad \text{otherwise} \end{cases} \qquad (4)$$

where ε_{bs} and $\sigma_{bs} = 1/2(\sigma_b + \sigma_s)$ establish the energy and length scales of the potential, respectively, and κ_{bs} is the reduced interaction range or screening parameter. We consider both the attractive and repulsive Yukawa tail because both types of interactions are manifested in real colloidal dispersions.

2. 2. Monte Carlo Simulations

2. 2. 1. Structure and Thermodynamics

For the CS model of Eq. 1 we performed Grand Canonical Ensemble Monte Carlo (GCEMC) simulations at constant chemical potential μ, volume *V*, and temperature *T*. This set of independent parameters that define the thermodynamic state of the system made possible the study of equilibrium between the bulk CS fluid and that subjected to external fields originating from the presence of various spatial constrains. For the latter, we have chosen a hard flat interface and a pair of parallel plates mimicking a planar pore. The general features of the GCEMC method are described elsewhere.[34] In the present study we determined some thermodynamic properties following from the simulation of bulk CS fluid. The excess internal energy U^{ex} results directly from simulations as it is equal to ensemble average of the potential energy. The reduced excess Helmholtz free energy has been calculated from the general expression

$$\frac{A^{ex}}{\langle N \rangle kT} = \frac{\mu_b^{ex}}{kT} - Z + 1 \qquad (5)$$

where the reduced excess chemical potential of the bulk fluid μ_b^{ex}/kT (*k* stands for the Boltzmann constant) is one of the input parameters, while the bulk density ρ_b and the compressibility factor $Z = P/\rho_b kT$ result from the open ensemble simulation. The bulk pressure *P* has been calculated using virial equation,[35] which involves the integration over the first derivative of the interparticle potential, φ(r). As discontinuous CS potential given by Eq. 1 can be written as a sum of Heaviside step-functions the derivative φ(r) gives a set of Dirac δ functions. Integration over this set finally yields:

$$Z = \frac{P}{\rho_b kT} = 1 + \frac{2\pi\rho_b}{3}\left\{\sigma^3 \cdot g(\sigma_+) + b^3 \cdot \right.$$
$$\left. \cdot\left[g(b_+) - g(b_-)\right] + c^3 \cdot \left[g(c_+) - g(c_-)\right]\right\} \qquad (6)$$

where $g(\sigma_+)$, $g(b_+)$, $g(b_-)$, etc. represent extrapolated values of the radial distribution function *g*(r) at the discontinuity points of the CS potential. Subscripts (+) and (–)

denote extrapolation to these points from the right and from the left, respectively. Further, we estimated also the isothermal compressibility, which is related to the fluctuations of the number of particles during the open ensemble simulation:[35]

$$\kappa_T = \frac{V}{\langle N \rangle kT}\frac{\langle N^2 \rangle - \langle N \rangle^2}{\langle N \rangle} \qquad (7)$$

where $\langle N \rangle/V$ is the average bulk density.

2. 2. 2. Effective Forces Between a Pair of Colloids

Solvent mediated force between a pair of colloidal particles was calculated by carrying out standard *N, V, T* ensemble (constant number of particles, volume and temperature) Monte Carlo (MC) simulations[34] with periodic boundary conditions in all three directions. This canonical simulation setup contained two big spheres fixed at prescribed positions along the body diagonal of the cubic MC box and small mobile particles of the CS fluid. The length of the box $L = 20\sigma_s$ was sufficient to avoid any pronounced periodic image effects.

The mean force between two macroparticles at prescribed center-to-center separations was calculated applying a simulation technique based on a separate sampling of the contributions arising from the Yukawa tail and hard-core parts of the big-small interaction potential to the total inter-colloidal force.[25,26] According to this method, the total force between a pair of big particles F_{bb}(r) is written as a sum of individual contributions,[25,26]

$$F_{bb}(r) = -\frac{\partial\phi_{bb}(r)}{\partial r} - \left\langle\sum_{i=1}^{N}\frac{\partial\phi_{bs}(r_{bs})}{\partial r}\right\rangle + F_{hs}(r) \qquad (8)$$

stemming from the interaction of big particles among themselves and that arising from the interactions with small solvent molecules. The first term on the right hand side of Eq. 8 is the direct big-big interaction. In our case, this contribution is zero as we set $\phi_{bb} = 0$. The second term comprises the big-small interactions arising from the tail part of the big-small interaction potential ϕ_{bs}. This contribution can be directly sampled in a MC simulation, the angular brackets denoting ensemble average. The last term, which represents the mean force due to the collisions between the macroparticles and neighboring molecules of the solvent, cannot be directly sampled in a simulation. The essence of this method[25,26] is just a special procedure derived for the calculation of the hard-sphere collision force. As demonstrated in the studies of Refs. 25 and 26, the collision force can be determined from the difference in average numbers of big-small collisions due to small trial displacements of big particles in either direction on the vector connecting their centers. For details of this procedure we refer the reader to the original works of Refs. 25 and 26.

3. Numerical Results and Discussion

Investigation of the phase behavior of the homogeneous CS model system for various combinations of potential parameters was given in a recent study of Skibinsky et al.[21] Therein, the authors used the event-driven molecular dynamics simulation, which enables a treatment of the discontinuous step-wise potentials, to determine the corresponding phase diagrams. The results were presented by the two-phase coexistence curves in the pressure-density $(P - \rho)$ planes. It was found that for a broad range of parameters the isotropic CS system has a phase diagram with a gas-liquid critical point C_1 and a liquid-liquid critical point C_2, separating high density liquid (HDL) and low density liquid (LDL) phases. The critical values for both C_1 and C_2 were estimated as the points where the maxima of coexistence and spinodal curves coincide. In this present study all calculations are carried out at one set of reduced ranges (in units of σ) of the CS potential given by Eq. 1, $b = 1.5$, $c = 2$, and at fixed value of the energy parameter $\lambda = 2$, which means that the height of the repulsive shoulder is twice as much as the depth of the attractive well. In the following discussion, we measure density, pressure, and temperature in units of σ^{-3}, $\varepsilon\sigma^{-3}$, and ε/k, respectively. The corresponding reduced quantities are denoted as $\rho^* = \rho_b\sigma^3$, $P^* = P\sigma^3/\varepsilon$, and $T^* = kT/\varepsilon$. The values for critical points C_1 and C_2 for the above set of potential parameters were assessed as $T^*_{c1} = 0.96 \pm 0.01$, $\rho^*_{c1} = 0.11 \pm 0.01$ and $T^*_{c2} = 0.53 \pm 0.03$, $\rho^*_{c2} = 0.39 \pm 0.05$.[21]

3. 1. Structure and Thermodynamics

The simulation results for the structure of CS fluid in various physical situations are presented in Figures 1–3. The calculations were carried out at the temperatures close to both critical values, i.e., for $T = 1.05 \cdot T_{c1}$ and $T = 1.05 \cdot T_{c2}$. In turn, Figure 1 displays the radial distribution function (RDF) $g(r)$ of the bulk CS fluid for the individual temperatures and at different densities, whereas Figures 2 and 3 show the one-particle distribution function $g_w(x) = \rho(x)/\rho_b$ for the same fluid at a single hard wall (Figure 2), and in a planar pore of width $H = 5\sigma$ (Figure 3). $\rho(x)$ is the density profile, which characterizes the spatial inhomogeneity of the fluid subjected to external field(s).

The shape of bulk RDFs shown in Figure 1 resembles that for the usual square-well fluid with the difference that it exhibits two step discontinuities at the distances coinciding with the ranges of the successive repulsive and attractive parts in the CS potential function. Its overall form stems from the interplay between the repulsive and attractive parts of the interaction potential. Of course, the expressiveness of these competitive influences strongly depends on the temperature and the density. At lower densities, for example, the molecules have a better chance to avoid the separations falling into the region of repulsive

shoulder leading to lower values of $g(r)$ at shorter intermolecular distances. At higher densities, however, the molecules are forced to occupy also the energetically unfavorable separations coinciding with the range of soft repulsion, which gives rise to higher contact values of $g(r)$. Similar features can be extracted also from some thermodynamic properties gathered in Table 1 for the temperature $T = 1.05 \cdot T_{c1}$. As the behavior of the CS fluid depends on a competition between the repulsive and attractive parts of the potential that further depends on the density of the system, the reduced excess thermodynamic functions, i.e., the internal energy $U^{ex}/\langle N \rangle kT$, Helmholtz free energy $A^{ex}/\langle N \rangle kT$, and chemical potential μ_b^{ex}/kT show
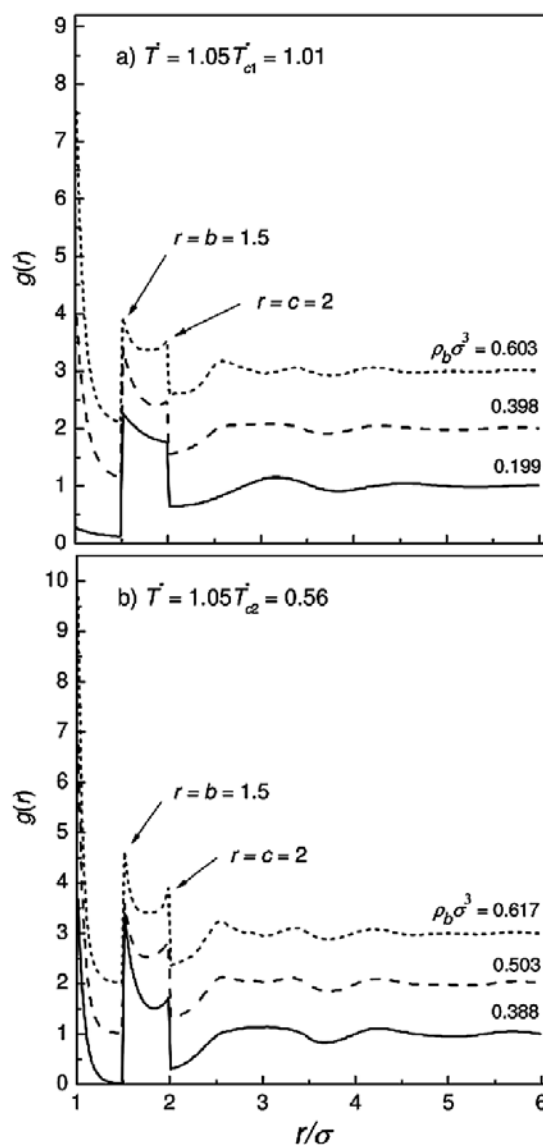

Figure 1. The bulk radial distribution function of the CS model fluid with the range parameters $b = 1.5$, $c = 2$ and the energy parameter $\lambda = 2$ at two temperatures, $T = 1.05 \cdot T_{c1}$ (a) and $T = 1.05 \cdot T_{c2}$ (b), and at different densities. For the reason of clarity, the data corresponding to individual densities are shifted upwards by adding different factors (0, 1 and 2).

Table 1. Thermodynamic properties of bulk CS fluid with the range parameters $b = 1.5$, $c = 2$ and the energy parameter $\lambda = 2$ at the reduced temperature $1.05 \cdot kT_{c1}/\varepsilon = 1.01$.

$\rho_b\sigma^3$	μ_b^{ex}/kT	$U^{ex}/\langle N\rangle kT$	$P\sigma^3/\varepsilon$	$Z = P/\rho_b kT$	$A^{ex}/\langle N\rangle kT$	$\kappa_T\varepsilon/\sigma^3$
0.101	−1.431	−2.048	0.039	0.384	−0.815	78.969
0.199	−1.776	−3.340	0.094	0.474	−1.250	2.265
0.299	0.707	−3.964	0.832	2.782	−1.075	0.330
0.398	2.921	−3.564	1.672	4.198	−0.277	0.309
0.504	5.085	−3.465	2.726	5.410	0.675	0.139
0.603	7.906	−3.311	4.327	7.179	1.727	0.082

extreme values at some intermediate density. On the other hand, the pressure and the compressibility factor grow monotonously with increasing the density. As expected, an increase of the compressibility coefficient is accompanied by a decrease of the isothermal compressibility shown in the last column of Table 1.
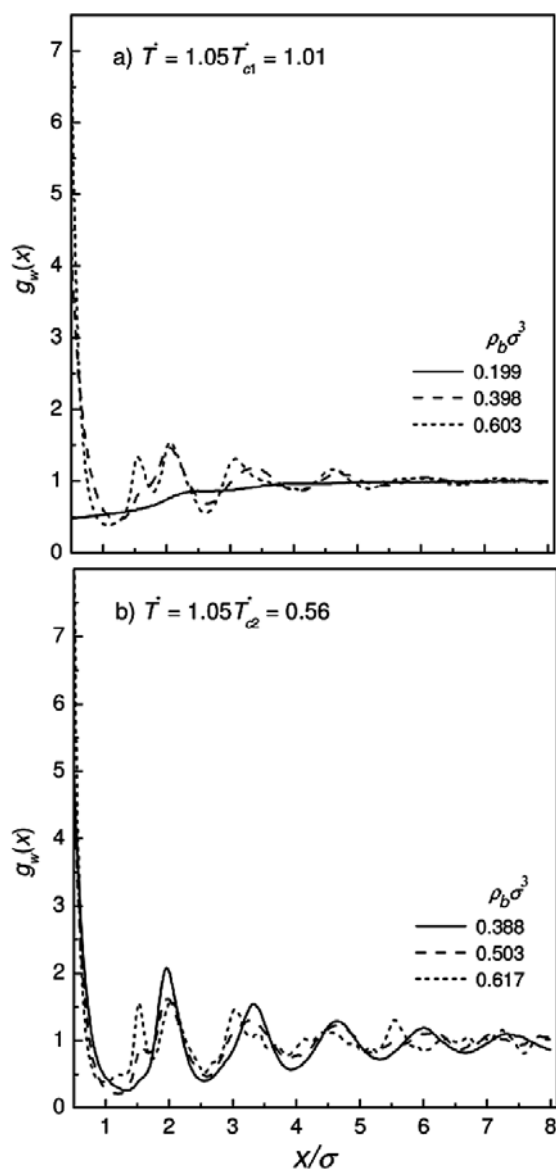

Figure 2. The one-particle distribution function of the CS fluid with the range parameters $b = 1.5$, $c = 2$ and the energy parameter $\lambda = 2$ near a single hard wall at two temperatures, $T = 1.05 \cdot T_{c1}$ (a) and $T = 1.05 \cdot T_{c2}$ (b), and at different densities of the equilibrium bulk fluid.
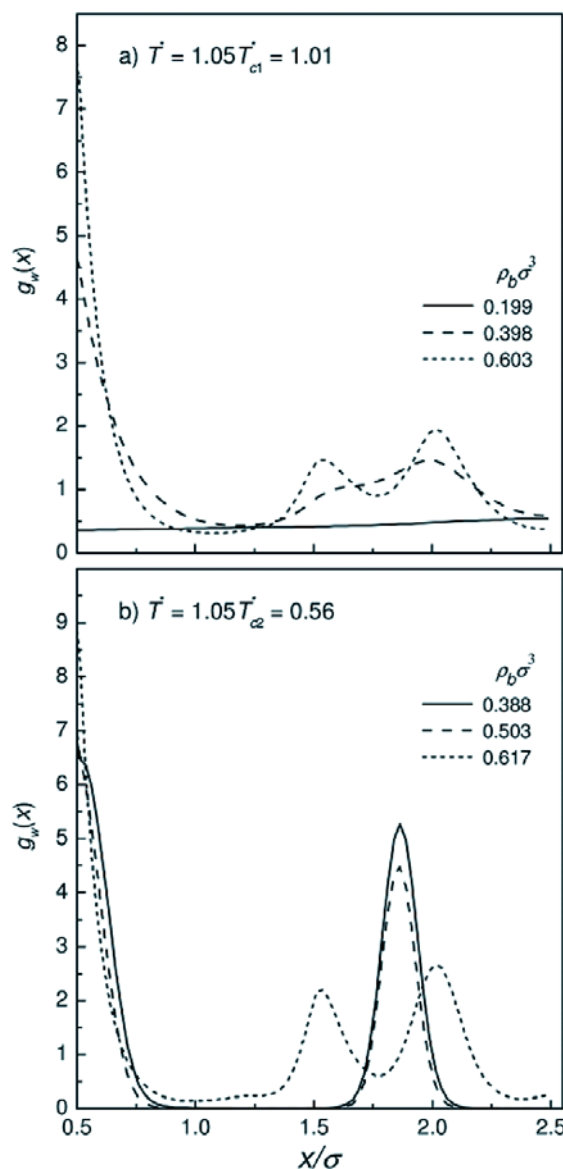
Figure 3. The single-wall one-particle distribution function of the CS fluid with the range parameters $b = 1.5$, $c = 2$ and the energy parameter $\lambda = 2$ in a planar pore of width $H = 5\sigma$ at two temperatures, $T = 1.05 \cdot T_{c1}$ (a) and $T = 1.05 \cdot T_{c2}$ (b), and at different densities of the equilibrium bulk fluid.

The results for the inhomogeneous structure of the CS fluid displayed in Figures 2 and 3 show characteristic structural features as reported by numerous articles in the literature dealing with the behavior of fluids at interfaces and in confined systems. A general feature found for the structure of the fluids was their spatial inhomogeneity as a consequence of the packing effects of fluid molecules in the domain close to the wall(s). The actual course of the density profiles, that characterize this inhomogeneity, depends on the specific nature of the fluid-fluid and the wall-fluid interactions, and on the degree and geometry of confinement. When an inhomogeneous structure of the fluid stem from the presence of a single wall, flat density profiles $\rho(x) = \rho_b$ (i.e. $g_w(x) = 1$) are restored at sufficient distances from the wall, irrespective of the specific nature of the intermolecular potential of interactions. Upon approaching the wall these interactions begin to compete with steric effects. This competition, of course, is now strongly dependent on the particular intermolecular potential and in addition, on the temperature of the system. In any case, the interactions among the molecules gain in importance upon lowering temperature. As the strongly attractive molecules have a better chance for mutual attraction at sufficient distances from the wall(s) or outside the confined system, they are driven away from the hard obstacles or toward the center of the micro-objects with restricted geometry (planar gap). As expected, just the opposite behavior has been observed for the molecules interacting through purely repulsive interaction potential. Clearly, strongly repulsive molecules try to avoid each other and as such they prefer the regions adjacent to the walls of the confinement. Such molecules are therefore accumulated next to the walls to a greater extent than those incorporating some attractive interactions thus giving rise to more pronounced packing effects leading to more distinct layering structure and higher wall-fluid contact density of the fluid with repulsive particles. As mentioned above the role of the interparticle interactions strengthens with reducing the temperature. For this reason, lowering temperature causes a decrease of the contact density and weaker oscillations in the density near the walls in the case of the model fluids with attractive molecules. Again, just the opposite holds for the fluid comprising purely repulsive particles. In summary, imposing of the qualitatively different interactions (attractive or repulsive) to the molecules of the fluid gives rise to qualitatively different redistributions of the molecules inside the confined system, leading to thermodynamically the most favorable structures in both cases. In the case of CS model incorporating both a soft repulsion and attractive interactions in the potential function one meets with a combination of all these effects. The resulting density profiles of confined CS fluid thus show the shapes arising from the complex interplay among the steric effects and the competition between the repulsive and attractive parts of the CS potential.

3. 2. Effective Inter-colloidal Force

We consider a pair of big (macro)spheres with the diameter $\sigma_b = 5\sigma_s$ (σ_s is the diameter of small CS molecules) fixed along the body diagonal in a cubic simulation box of length $L = 20\,\sigma_s$ with periodic boundary conditions imposed in all directions. Relatively large dimension of the MC box implies a huge number of solvent molecules, the actual number depending on the chosen density. We performed calculations for the two qualitatively different physical situations, i.e., for attractive and repulsive big-small interactions. In Eq. 4, the corresponding energy pa-
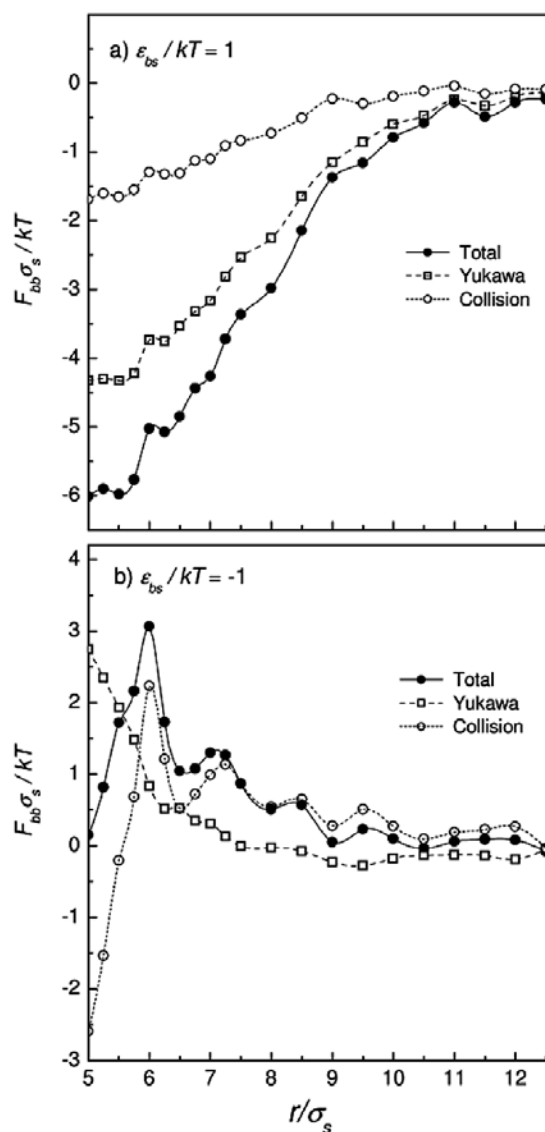

Figure 4. Mean force between a pair of big (colloidal) particles in the CS fluid with the range parameters $b = 1.5$, $c = 2$ and the energy parameter $\lambda = 2$ at the temperature $T = 1.1T_{c1}$ for two values of big-small interaction parameter, $\varepsilon_{bs}/kT = 1$ (a) and $\varepsilon_{bs}/kT = -1$ (b). Solid circles represent the total force, while the separate contributions are represented by squares (Yukawa tail interaction) and open circles (collision force), respectively. The lines are to guide the eye.

rameter is chosen as $\varepsilon_{bs}^{*} = \varepsilon_{bs}/kT = -1$ and $\varepsilon_{bs}^{*} = 1$, respectively, whereas the interaction range parameter κ_{bs} is fixed at 1.8. For all simulations the temperature is $1.1 \cdot T_{c1}$ and the solvent number density is set to 0.2. The force between macroparticles is sampled by carrying out separate canonical ensemble MC simulations for a set of fixed macroparticle-macroparticle distances. For this purpose, as briefly outlined in the previous section, we use a procedure described in detail in Refs. 25 and 26.

In Figure 4 we present the results for the effective force between the macrospheres mimicking colloidal particles for both types of big-small interactions, repulsion (Figure 4a) and attraction (Figure 4b). Similarly as observed in numerous studies of inter-colloidal forces exploring many different model systems[25,26,36–38] the big-small repulsion gives rise to more attractive forces, while the big-small attraction leads to more repulsive forces. In the former case the solvent molecules are driven away from the colloids resulting in a depletion layer around the big particles. At shorter inter-colloidal distances this effect is much more pronounced in the region between the colloidal particles where the solvent molecules are doubly repulsed by both big particles, thus giving rise to more attractive force. According to the origin of this effect, we usually speak about a depletion force and depletion interactions, respectively. Of course, just the opposite behavior is expected in the case of big-small attraction. In this case, the density of the solvent molecules in the accessible region between the adjacent big spheres exceeds the solvent density at the macroparticle surface opposite the neighboring macroparticle. This leads to an effective repulsion between the macroparticles, the features originating mainly by a net hard-sphere collision interaction. The overall situation is, of course, dependent also on the type and strength of small-small interactions, which are not varied in our case. However, as reported in other studies[36–38] dealing with similar systems, the dominant effect in this respect represents the big-small interaction whereas the change of the small-small interactions does not influence the qualitative picture significantly.

4. Conclusions

In this paper we have studied an isotropic attractive soft-core potential (denoted as core-softened (CS) model fluid), which has a phase diagram with a gas-liquid critical point C_1 and a liquid-liquid critical point C_2 separating high density liquid (HDL) and low density liquid (LDL) phases. First, we performed grand canonical ensemble Monte Carlo (MC) simulations to investigate the structure and thermodynamic properties of homogeneous and inhomogeneous CS fluid. The bulk radial distribution function $g(r)$ exhibits two step discontinuities at the positions coinciding with the ranges of the two successive discontinuous regions in the CS potential function. The structure of this

fluid at the planar interphase and confined in planar pore resemble those found for many other model fluids, the density profiles exhibiting the shapes arising from the complex interplay among the steric effects and the competition between the repulsive and attractive parts of the CS potential. In the second part of this study canonical MC simulation has been used to explore the effective force between a pair of big colloidal spheres (solute) immersed in a CS solvent. The solute-solvent interactions were modeled as hard core pair potentials with attractive or repulsive Yukawa tail mimicking lyophilic and lyophobic colloidal dispersions, respectively. The inter-colloidal force was calculated by applying a simulation technique developed for a separate determination of the contributions arising from the Yukawa tail part of the solute-solvent interaction potential and that stemming from the hard-core collisions of colloids with the molecules of the CS solvent (see refs. 25 and 26). As expected, the solute-solvent repulsive interactions give rise to net (depletion) attraction whereas the solute-solvent attractive interactions lead to net (accumulation) repulsion between the colloidal particles.

5. Acknowledgements

6. References

1. P. C. Hemmer, G. Stell, *Phys. Rev. Lett.* **1970**, *24*, 1284–1287.
2. G. Stell, P. C. Hemmer, *J. Chem. Phys.* **1972**, *56*, 4274–4286.
3. A. Ben-Naim: Statistical Thermodynamics for Chemists and Biochemists, Plenum Press, New York, **1992**.
4. F. H. Stillinger, T. Head-Gordon, *Phys. Rev. E* **1993**, *47*, 2484–2490.
5. C. H. Cho, S. Singh, G. W. Robinson, *Phys. Rev. Letters* **1996**, *76*, 1651–1654.
6. F. H. Stillinger, D. K. Stillinger, *Physica A* **1997**, *244*, 358–369.
7. E. A. Jagla, *Phys. Rev. E* **1998**, *58*, 1478–1486.
8. M. R. Sadr-Lahijany, A. Scala, S. V. Buldyrev, H. E. Stanley, *Phys. Rev. Lett.* **1998**, *81*, 4895–4898.
9. G. Franzese, G. Malescio, A. Skibinsky, S. V. Buldyrev, H. E. Stanley, *Nature* **2001**, *409*, 692–695.
10. S. V. Buldyrev: in New Kinds of Phase Transitions: Transformations in Disordered Substances, NATO Advanced Research Workshop, Volga River, V. Brazhkin, S. Buldyrev, V. Ryzhov, H. Stanley (Eds.), Kluwer, Dordrecht, **2002**.
11. S. V. Buldyrev, H. E. Stanley, *Physica A* **2003**, *330*, 124–129.

12. F. Franks: Water: A Comprehensive Treatise, *1–7,* Plenum Press, New York, **1972.**

13. F. Franks: Water Science Reviews, *1–4,* Cambridge University Press, Cambridge, **1985.**

14. M. G. Campos, J. R. Grigera, *Mol. Simul.* **2004,** *30,* 537–542.

15. P. H. Poole, F. Sciortino, U. Essmann, H. E. Stanley, *Nature* **1992,** *360,* 324–328.

16. O. Mishima, H. E. Stanley, *Nature* **1998,** *396,* 329–335.

17. F. Sciortino, E. La Nave, P. Tartaglia, *Phys. Rev. Lett.* **2003,** *91***,** art. no. 155701.

18. G. Franzese, G. Malescio, A. Skibinsky, S. V. Buldyrev, H. E. Stanley, *Phys. Rev. E* **2002,** *66,* art. no. 051206.

19. G. Malescio, G. Franzese, A. Skibinsky, S. V. Buldyrev, H. E. Stanley, *Phys. Rev. E* **2005,** *71,* art. no. 061504.

20. S. Zhou, A. Jamnik, E. Wolfe, S. V. Buldyrev, *Chem Phys Chem* **2007,** *8,* 138–147.

21. A. Skibinsky, S. V. Buldyrev, G. Franzese, G. Malescio, H. E. Stanley, *Phys. Rev. E* **2004,** *69,* art. no. 061206.

22. R. Tuinier, J. Rieger, C. G. de Kruif, *Adv. Colloid Interface Sci.* **2003,** *103,* 1–31.

23. W. C. K. Poon, *J. Phys.: Condens. Matter* **2002,** *14,* R859–R880.

24. Y. Snir, R. D. Kamien, *Science* **2005,** *307,* 1067–1067.

25. J. Wu, D. Bratko, J. M. Prausnitz, *Proc. Natl. Acad. Sci.* **1998,** *95,* 15169–15172.

26. J. Wu, D. Bratko, H. W. Blanch, J. M. Prausnitz, *J. Chem. Phys.* **1999,** *111,* 7084–7094.

27. P. R. tenWolde, D. Frenkel, *Science* **1997,** *277,* 1975–1978.

28. S. Auer, D. Frenkel, *Nature* **2001,** *409,* 1020–1023.

29. F. H. Stillinger, T. Head-Gordon, *Phys. Rev. E* **1993,** *47,* 2484–2490.

30. F. H. Stillinger, D. H. Stillinger, *Physica A* **1997,** *244,* 358–369.

31. D. Wei, G. N. Patey, *Phys. Rev. Lett.* **1992,** *68,* 2043–2045.

32. S. H. Behrens, D. I. Christl, R. Emmerzael, P. Schurtenberger, M. Borkovec, *Langmuir* **2000,** *16,* 2566–2575.

33. F. Lo Verso, M. Tau, L. Reatto, *J. Phys.: Condens. Matter* **2003,** *15,* 1505–1520.

34. D. Frenkel, B. Smit: Understanding Molecular Simulation, Academic Press, Boston, MA, **1996.**

35. J. P. Hansen, I. R. McDonald: Theory of simple liquids, Academic Press, London, **1986.**

36. E. Allahyarov, H. Löwen, S. Trigger, *Phys. Rev. E* **1998,** *57,* 5818–5824.

37. E. Allahyarov, H. Löwen, *Phys. Rev. E* **2001,** *63,* art. no. 041403.

38. A. A. Louis, E. Allahyarov, H. Löwen, R. Roth, *Phys. Rev. E* **2002,** *65,* art. no. 061407.

Povzetek

Z računalniško simulacijo Monte Carlo smo obravnavali modelno tekočino z mehkim odbojnim medmolekulskim potencialom (angl. 'core-softened (CS) fluid'). Taka tekočina ima poleg običajne kritične točke para-kapljevina še kritično točko, ki loči dve kapljevinasti fazi z različnima gostotama. V prvem delu smo z velekanonično simulacijo proučevali termodinamske in strukturne lastnosti homogene tekočine ter njeno strukturo v mikropori. Meddelčna radialna porazdelitvena funkcija je pri razdaljah, ki sovpadata z dosegom odbojnega in privlačnega dela medmolekulskega potenciala interakcije, nezvezna. Oblika gostotnih profilov v mikropori je posledica zapletenih vzajemno delujočih interakcij stena-molekule ter privlačnega in odbojnega dela medmolekulske interakcije. V drugem delu smo določali silo med velikima kroglama, ki sta ponazarjala par koloidnih delcev (topljenec), v CS topilu. Interakcije topljenec-topilo smo obravnavali s parskim potencialom, ki poleg togega odbojnega 'jedra' vključuje še Yukawin privlačni ali pa odbojni 'rep'. Silo smo računali z uporabo posebne tehnike kanonične simulacije, ki omogoča ločeno vzorčenje posameznih prispevkov (togega jedra in privlačnega oz. odbojnega repa) interakcije koloid-molekule topila na silo med koloidnima delcema. V skladu s pričakovanji, odbojne interakcije koloid-molekule topila vodijo do privlačne sile med koloidnima delcema (angl. 'depletion force'), privlačne interakcije pa povzročijo odbojno silo.